Journal of Hydroscience and Hydraulic Engineering
Vol. 19, No.2 November, 2001, 93-104

FUNDAMENTAL STUDY ON DIRECT NUMERICAL SIMULATION USING A HIGH-ORDER ACCURACY UPWIND DIFFERENCE SCHEME

By

Shunichiro Hayashi

Department of Civil Engineering, Kumamoto Prefectural Government,
6-18-1 Suizenji, Kumamoto, Japan

Terunori Ohmoto

Associate Professor, Department of Civil and Environmental Engineering,
Kumamoto University, 2-39-1 Kurokami, Kumamoto, Japan

and

Kiyoshi Takikawa

Professor, Research and Education Center of Coastal Environmental Science,
Kumamoto University, 2-39-1 Kurokami, Kumamoto, Japan

SYNOPSIS

Studies were conducted using Direct Numerical Simulation (DNS) with an upwind difference scheme and regular mesh to investigate its applicability to complex boundary and high Reynolds number flows. A one-dimensional linear advection equation was calculated by using the upwind scheme in combination with time marching schemes. The results showed that a 5th-order accurate upwind scheme for the convective term and the 3rd-order Adams-Bashforth method for time marching was the most accurate and stable among the combinations investigated. Furthermore, fully developed turbulent flows between parallel plates were analyzed to clarify the influence of various difference schemes on computational accuracy of convective terms. Comparisons with the spectral method revealed that the high-order upwind DNS is sufficiently accurate with respect to turbulence statistics.

INTRODUCTION

Advancements in the understanding of chaos reveal that many physical systems which show irregular temporal and spatial behavior are governed by deterministic equations. This means that fluid phenomena can be reproduced quantitatively by solving Navier-Stokes equations[18]. Numerous attempts have been made in recent years to simulate turbulent flows through numerical analysis[6]. Among the various methods proposed thus far, direct numerical simulation (DNS) by far excels others in terms of reliability and analytical accuracy. Early attempts at applying DNS often used the spectral method, but this approach does not make use of all the advantages of DNS. In recent years, therefore, attempts have been made to use finite difference schemes because of their applicability to more complex boundaries. Although most of these attempts are based on second-order accuracy, there are some that have been shown to be as accurate as the spectral method[17].

A common method of calculating for high Reynolds number flows is to use a pseudo-direct method using a third-order upwind difference scheme[5]. Because of its high numerical stability, schemes of this type are widely adopted for general-purpose software intended mainly for practical calculations like flows around an arbitrarily shaped body. One of the reasons for this trend is that in the analysis of high Reynolds number flows, the use of a central difference scheme tends to lead to nonlinear instability, in spite of high-order accuracy, because leading truncation error terms become odd-order derivatives, thus making

it necessary to use a numerical filter such as an upwind difference scheme to remove high waver number components. However, the influence of numerical viscosity of such a scheme on solutions has been pointed out[8], and many studies have already been conducted to investigate this matter.

In the area of turbulent flow analysis, Rai and Moin[16] proposed a fifth-order upwind difference scheme. Miyauchi et al.[12] applied the scheme to homogeneous isotropic turbulent flows and reported that their results agreed well with laboratory experiments and spectral method results. DNS combined with upwind schemes, therefore, may become applicable to more practical problems. In view of the difficulties associated with the analysis of high Reynolds number flows, which are important in engineering, it is necessary to use some kind of numerical filter, such as upwind difference schemes, while considering its influence. Therefore, investigating the influence of upwind difference schemes on the accuracy of solutions is very important from an engineering standpoint .

In this study, we consider one-dimensional linear convection problems to show the importance of an appropriate combination of an upwind difference scheme and the temporal discretization method. Quantitative evaluation is also taken on characteristics of the DNS method combining an upwind difference scheme and a regular grid applied to flows between two parallel plates -- a typical problem used for verification of applicability of the DNS method to wall-shear turbulent flows.

SELECTING A COMBINATION OF UPWIND DIFFERENCE AND TIME ADVANCEMENT SCHEMES

Just as solutions diverge because of aliasing errors if a nonconservative central difference scheme is used, stable solutions cannot be obtained unless a special preventive measure is taken with respect to the convection terms, which are nonlinear. The upwind difference method is a means of removing such instability. In this section, the influence of the coupling of an upwind different and a time advancement scheme on solutions is investigated by applying it to the one-dimensional linear convection problem:

$$\frac{\partial u}{\partial t}+U\frac{\partial u}{\partial x}=0, \qquad (U=1,\ -\infty<x<\infty)$$
$$u(x,0)=\begin{cases}\dfrac{1-\cos(2x-\pi)}{2}, & (\dfrac{\pi}{2}\le x\le\dfrac{3\pi}{2})\\ 0, & otherwise\end{cases} \tag{1}$$

Adequacy of numerical viscosity of an even-order derivative type, in addition to amplitude and phase errors, is examined by adopting a function that is smooth for the initial value but has discontinuous even-order derivatives at $\pi/2$ and $3\pi/2$ [2]. As the initial values of this problem are conserved, an equally spaced grid ($N=65$) is used in the analysis, and numerical and exact solutions at the time of return to the original position after m cycles are compared by adopting periodic boundary conditions at both ends. For convection term approximations, five methods, namely, first-order upwind scheme, third-order upwind schemes (K-K,[5] UTOPIA,[9] QUICK[10]), and fifth-order upwind scheme shown in Eqs.2 to 6 are used. Four time integration methods are used, namely, Crank-Nicolson, Runge-Kutta, second-order Adams-Bashforth, and third-order Adams-Bashforth. Numerical experiments are carried out using combinations shown in Table 1.

1) First-order upwind

$$\left(u\frac{\partial u}{\partial x}\right)_i = u_i\frac{u_{i+1}-u_{i-1}}{2\Delta x} + |u_i|\frac{-u_{i+1}+2u_i-u_{i-1}}{2\Delta x} \tag{2}$$

2) K-K scheme

$$\left(u\frac{\partial u}{\partial x}\right)_i = u_i\frac{-u_{i+2}+8(u_{i+1}-u_{i-1})+u_{i-2}}{12\Delta x} + |u_i|\frac{u_{i+2}-4u_{i+1}+6u_i-4u_{i-1}+u_{i-2}}{4\Delta x} \tag{3}$$

3) UTOPIA scheme

$$\left(u\frac{\partial u}{\partial x}\right)_i = u_i\frac{-u_{i+2}+8(u_{i+1}-u_{i-1})+u_{i-2}}{12\Delta x} + |u_i|\frac{u_{i+2}-4u_{i+1}+6u_i-4u_{i-1}+u_{i-2}}{12\Delta x} \tag{4}$$

4) QUICK scheme

$$\left(u\frac{\partial u}{\partial x}\right)_i = u_i \frac{-u_{i+2}+10\left(u_{i+1}-u_{i-1}\right)+u_{i-2}}{16\Delta x} + |u_i| \frac{u_{i+2}-4u_{i+1}+6u_i-4u_{i-1}+u_{i-2}}{16\Delta x} \tag{5}$$

5) Fifth-order upwind

$$\left(u\frac{\partial u}{\partial x}\right)_i = u_i \frac{u_{i+3}-9u_{i+2}+45\left(u_{i+1}-u_{i-1}\right)+9u_{i-2}-u_{i-3}}{60\Delta x} + |u_i| \frac{-u_{i+3}+6u_{i+2}-15u_{i+1}+20u_i-15u_{i-1}+6u_{i-2}-u_{i-3}}{60\Delta x} \tag{6}$$

Table 1:Combinations of Numerical Experiments

CASE		Time Marching	Convection term Approximation				
			1st.	K-K	UTOPIA	QUICK	5th.
RUN 1	①	Crank-Nicolson	○				
	②			○			
	③				○		
	④					○	
	⑤						○
RUN 2	①	Runge-Kutta	○				
	②			○			
	③				○		
	④					○	
	⑤						○
RUN 3	①	2nd Adams-Bash forth	○				
	②			○			
	③				○		
	④					○	
	⑤						○
RUN 4	①	3rd Adams-Bash forth	○				
	②			○			
	③				○		
	④					○	
	⑤						○

Figure 1 shows wave height damping (A) and amplitude errors (B), expressed in terms of the square root of the square residual. As shown in Figure 1(A), the lower-order upwind difference schemes show greater damping, regardless of the time advancement scheme used. Figure 1(B) shows that except for the first-order upwind scheme, which shows complete damping, the rates of growth of amplitude error indicated by the third-order upwind schemes are higher. Moreover, the fifth-order upwind scheme, whose amplitude errors are smallest, reveals little wave height damping, irrespective of the time advancement scheme used.

Table 2 summarizes amplitude errors after 50 cycles, shown in relation to the Courant number. RUN1 results show that the Crank-Nicolson method, which is an implicit solution scheme, gives stable solutions without causing solutions to diverge. In contrast, In the explicit solution schemes used in RUN2 to RUN4, solutions diverge unless the Courant number is limited to small values, particularly when the higher-order time advancement schemes are used. It should be noted that combination with a fifth-order upwind difference scheme seems to result in reduced amplitude errors and increased stability. Thus, regardless of the time advancement scheme selected, the use of a fifth-order scheme seems to contribute to a dramatic improvement of results.

Examination of the waveform results after 50 cycles shown in Figure 2 reveal, however, that all methods except the third-order Adams-Bashforth method in RUN4-⑤ show deviations, such as those indicated by negative values at points of discontinuity in even-order derivatives. In particular, the results of the second-order Adams-Bashforth method in RUN3-⑤ show Courant number dependence in addition to damping errors and phase errors (C is the Courant number in this figure). In contrast, the third-order Adams-Bashforth method is almost free of these problems. Furthermore, as the computational load of the third-order Adams-Bashforth method is smaller than that of the Crank-Nicolson method (which requires iterative calculations) and the multistep Runge-Kutta method, the third-order scheme should be useful in cases where it is necessary to perform calculations for a large number of time steps maintaining high accuracy in a DNS computation. In view of the fact that the number of integration time steps increases in proportion to $Re^{1/2}$ [4]. The use of the third-order Adams-Bashforth method can probably contribute to a

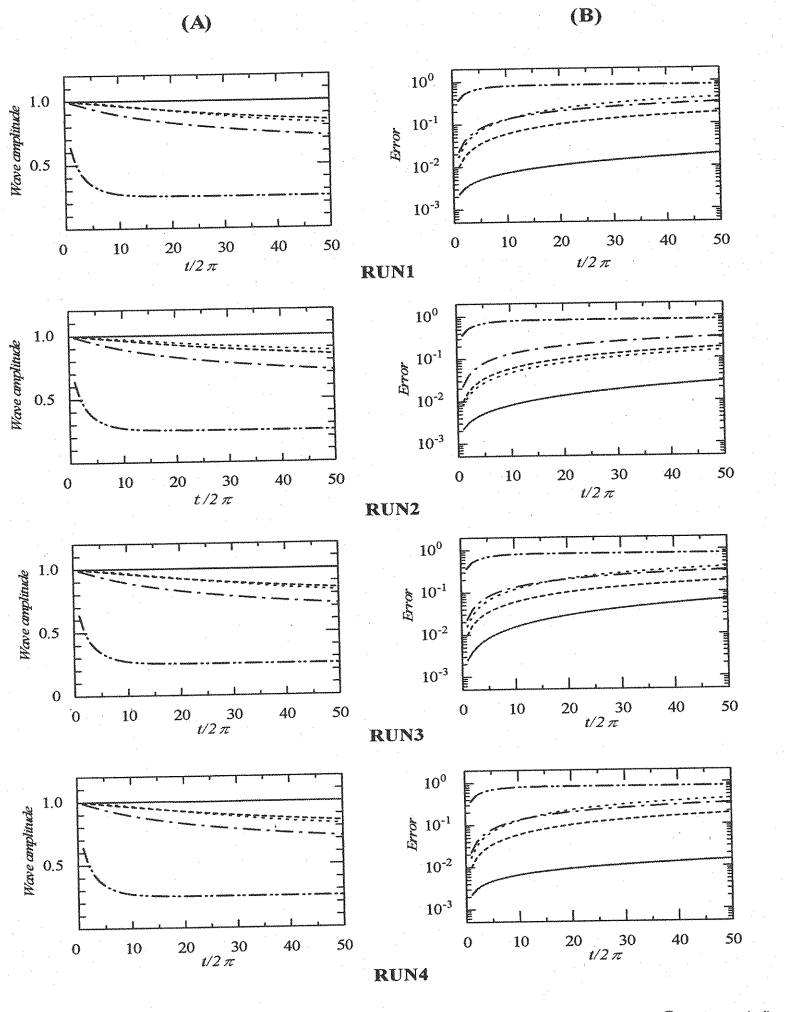

Figure 1 Comparison of wave amplitude and error

Table 2 State of amplitude errors after 50cycles

RUN1	Courant Number				
	0.1	0.2	0.3	0.5	1.0
① 1st-upwind	▲	▲	▲	▲	▲
② K-K	▲	▲	▲	▲	▲
③ UTOPIA	▲	▲	▲	▲	▲
④ QUICK	▲	▲	▲	▲	▲
⑤ 5th-upwind	○	○	▲	▲	▲

RUN2	Courant Number				
	0.1	0.2	0.3	0.5	1.0
① 1st-upwind	▲	▲	▲	▲	▲
② K-K	▲	▲	▲	▲	–
③ UTOPIA	▲	▲	▲	▲	–
④ QUICK	▲	▲	▲	–	–
⑤ 5th-upwind	○	▲	▲	–	–

RUN3	Courant Number				
	0.1	0.2	0.3	0.5	1.0
① 1st-upwind	▲	▲	▲	▲	–
② K-K	▲	▲	–	–	–
③ UTOPIA	▲	▲	▲	▲	–
④ QUICK	▲	▲	▲	–	–
⑤ 5th-upwind	○	○	▲	–	–

RUN4	Courant Number				
	0.1	0.2	0.3	0.5	1.0
① 1st-upwind	▲	▲	–	–	–
② K-K	▲	–	–	–	–
③ UTOPIA	▲	▲	▲	–	–
④ QUICK	▲	▲	▲	–	–
⑤ 5th-upwind	○	○	○	–	–

○ : Error less than 10^{-1} , ▲ : Error more than 10^{-1} , — : Divergence

dramatic reduction in computational load, particularly when analyzing high Reynolds number flows. For the purposes of this study, therefore, the third-order accurate Adams-Bashforth method is used as the time advancement scheme.

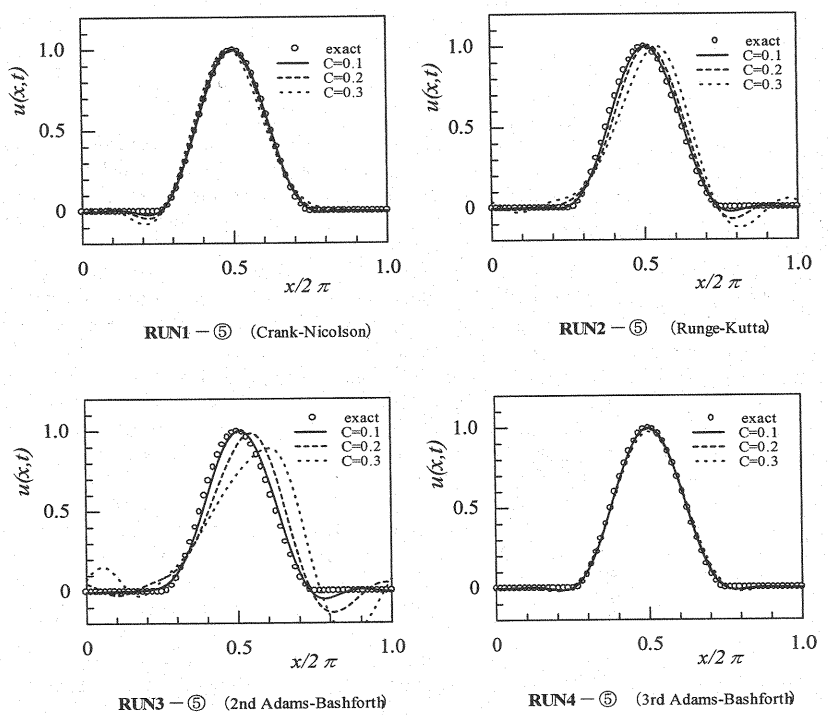

Figure 2 Comparison of time marching method after 50 cycles

NUMERICAL ANALYSIS METHOD

The equations governing incompressible viscous flows consist of the continuity and Navier-Stokes equations.

$$div\, U = 0 \tag{7}$$

$$\frac{\partial U}{\partial t} + (U \cdot \nabla) U = -grad\, p + \frac{1}{\mathrm{Re}} \nabla^2 U \tag{8}$$

where U is velocity vector; p, pressure; and Re, the Reynolds number. The above equations are analyzed using an algorithm combining the MAC method and the fractional step method[6], which is described below. A major characteristic of this algorithm is that it combines compactness due to an explicit scheme, convergence and numerical stability due to an implicit scheme, by expressing the nonlinear term of the evolution equation by the third-order Adams-Bashforth method (explicit) and the linear viscosity term by the second-order Crank-Nicolson method (implicit), and reduction of the overall method of solution due to separation of velocity and pressure.

$$\frac{\tilde{U}-U^n}{\Delta t}=\frac{1}{12}\left(23H^n-16H^{n-1}+5H^{n-2}\right)+\frac{1}{2\mathrm{Re}}\nabla^2\left(\tilde{U}+U^n\right) \tag{9}$$

$$\nabla^2 p^{n+1}=\frac{div\,\tilde{U}}{\Delta t} \tag{10}$$

$$\frac{U^{n+1}-\tilde{U}}{\Delta t}=-grad\,p^{n+1} \tag{11}$$

where H represents the convection terms, and n expresses time level. The Poisson equation for pressure is discretized to fourth-order accuracy, and velocity fields for new steps are calculated by applying the backward Euler scheme. The plane Gauss-Seidel method is used as the iterative solution for the Crank-Nicolson method in the Poisson equation for pressure and the Navier-Stoke equation. The convergence criteria are 10^{-4} and 10^{-9}, respectively, in terms of mean square residuals.

Staggered grids have often been used for calculation. However, the use of a staggered grid involves complicated programming including the definition of boundary conditions, and extension to generalized curvilinear coordinate systems and improvement of accuracy requires an ingenious approach.[1] Regular grids often have problems --spatial oscillation (spurious error) of solutions[14]-- but the use of a regular grid is advantageous in that programming is simple and conversion to a generalized curvilinear coordinate system which facilitates the treatment of complex boundaries is easy because physical quantities are defined at the same points. Because of these considerations, the use of a grid system that is compact and easy to handle is an important factor in facilitating the development of generally applicable DNS techniques. For the purposes of this study, therefore, a regular grid approach is adopted, and its applicability is demonstrated. An unequally spaced grid is adopted to prevent oscillation of numerical solutions. Since, however, the properties of high Reynolds number flows are not heavily dependent on the Reynolds number, except in the vicinity of the wall boundary, a relatively sparse grid is used in this low-dependence region. This arrangement may result in improvement of simulation efficiency as well as the elimination of oscillating solutions. In order to generate an unequally spaced grid, the hyperbolic function (tanh function) shown in Figure 3 is used to prevent the inclusion of errors due to coordinate transformation since metrics associated with mapping into the computational space are computed analytically. Since a dense grid can be defined in the near-wall region by adjusting α. α=2.5 was adopted so that about one-fourth of all grid points are defined in the viscous sublayer and the buffer layer. The computation involved mapping the governing equations into the computational space followed by difference approximation.

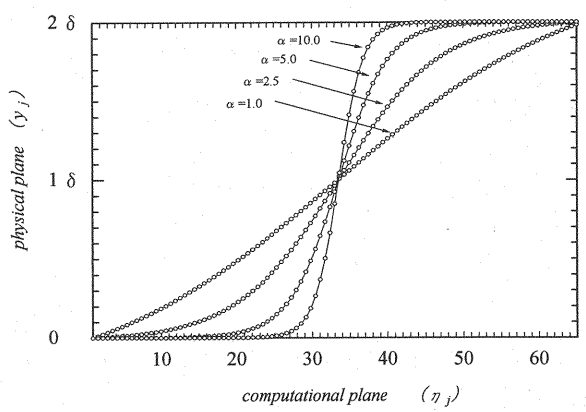

Figure 3 Coordinate transformation

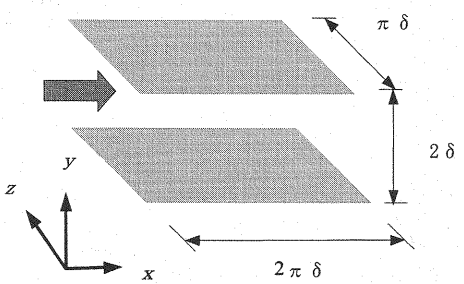

Figure 4 Flow configuration

Table 3 Conditions for calculation

Coupling algorithm	Fractional Step Method
Time advancement	3rd-order Adams-Bashforth
Spatial scheme	3rd-upwind (Convective term)
	5th-upwind (〃)
	2nd-central (〃)
	4th-central (〃)
	6th-central (〃)
	2nd-central (Viscous term)
Grid numbers	64×65×64 (regular)
Spatial resolution	$\Delta x^+ = 18$
	$\Delta y^+ = 0.45 \sim 13.9$
	$\Delta z^+ = 9$
Reynolds number	Rec = 3300
Time step	$\Delta t = 2/1000 * \delta / u_\tau$
Total steps	N = 100000

VERIFICATION OF ACCURACY

Flow between two parallel plates, as shown in Figure 4, was chosen as an example of calculation because it has a simple boundary configuration, which is convenient for examining the elementary process of wall-shear turbulent flow, and because a good database[3] based on the spectral method is available. As boundary conditions, the no-slip and Neumann boundary conditions are used for velocity and pressure, respectively, for the upper and lower surfaces. Periodic boundary conditions are specified for the streamwise and transverse directions. It is assumed that flows are driven by the constant mean pressure gradient, and a Reynolds number of 3300 is used for the flow velocity at the channel center and the channel half-width. Other conditions for calculation are shown in Table 3. A well-developed turbulence field is given as the initial value, and judgments as to the degree of development of the turbulence field were made by the degree of development and steadiness of turbulence statistics such as skewness and flatness. The Courant number[7] defined by Eq. 12 was smaller than 0.05 for all calculations.

$$C(t) = \max \left\{ \Delta t \left(\frac{|u|}{\Delta x} + \frac{|v|}{\Delta y} + \frac{|w|}{\Delta z} \right) \right\} \tag{12}$$

The difference schemes evaluated are the third- and fifth-order upwind difference schemes. However, because an upwind scheme can be expressed as the sum of central difference and numerical viscosity, the central difference results are also examined by eliminating the numerical viscosity term.

RESULTS AND DISCUSSION

Figures 5 and 6 compare the mean velocity distribution and turbulence intensity results with corresponding results obtained by the spectral method[3]. As shown, the values of mean velocity in the viscous sublayer agree well with those of the spectral method. Differences in the order of difference accuracy, however, begin to increase considerably in the vicinity of the buffer layer, and the fifth-order upwind results are slightly greater than the spectral method results in the logarithmic law region. In contrast, the third-order upwind results are much greater than the spectral method results due to numerical viscosity. As for turbulence intensity, however, the third-order upwind difference scheme overestimates u^+_{rms} and underestimates v^+_{rms}, indicating that there may be some problems associated with redistribution. This suggests that numerical viscosity does not necessarily cause laminar flow increases uniformly. The fifth-order upwind difference scheme results show close agreement in terms of v^+_{rms} and w^+_{rms}, although there are deviations in u^+_{rms} peak values. In view of the fact that the number of grid points is only about one-eighth of that used in the spectral method, these results may be considered satisfactory.

Figure 7 shows the distribution of Reynolds stresses and total shear stresses. As shown, differences between the third- and fifth-order upwind difference scheme results are small and agree sufficiently well with the spectral method results.

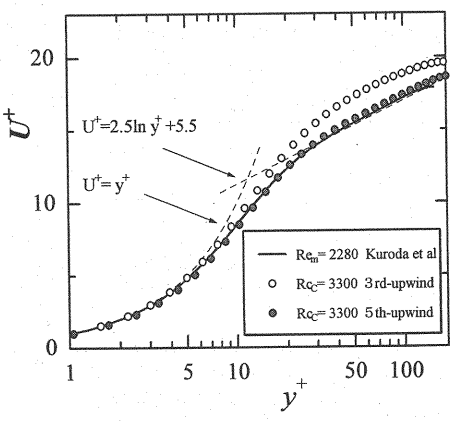

Figure 5 Mean velocity distribution

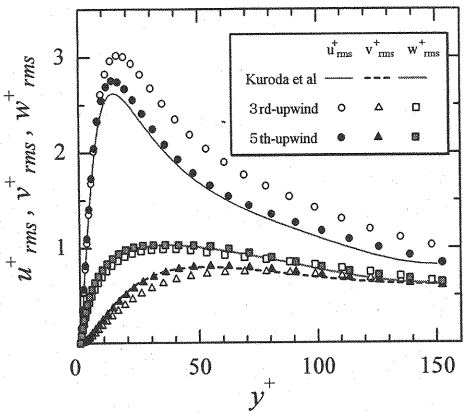

Figure 6 Turbulence intensity

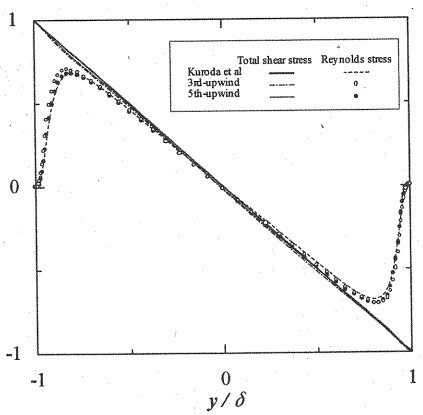

Figure 7 Reynolds stress

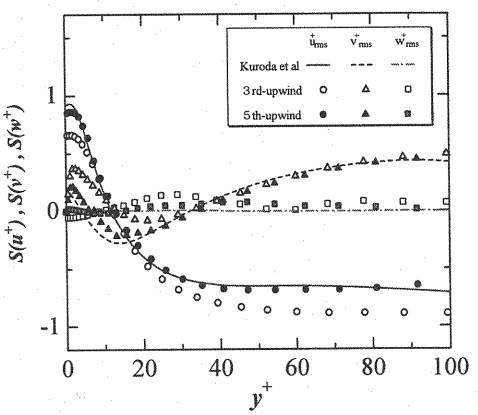

Figure 8 Skewness

Figures 8 and 9 show the skewness and flatness results, which are triple and quadruple correlations, respectively, of velocity fluctuations. In Figure 8, the skewness of x-direction velocity fluctuation changes reverses from positive to negative as the distance from the near-wall region increases, while that of y-direction velocity fluctuation reverses almost in the opposite direction. This indicates that sweeps due to the incoming high-speed fluid are dominant in the near-wall region, and ejections due to the flotation of low-speed fluid are dominant in the logarithmic-law region. Figure 9 accurately reproduces strong intermittency in the near-wall region, suggesting the existence of coherent structures such as bursting. Both Figures 8 and 9 accurately capture the deviations

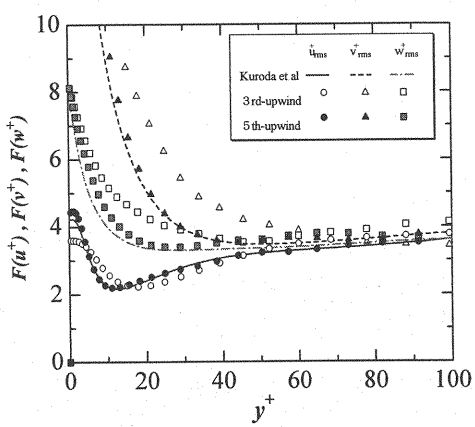

Figure 9 Flatness

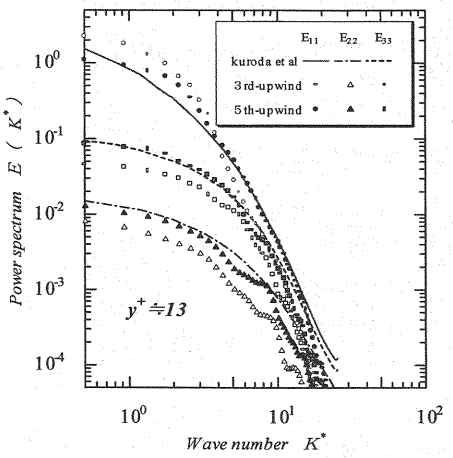

Figure 10 Energy spectrum

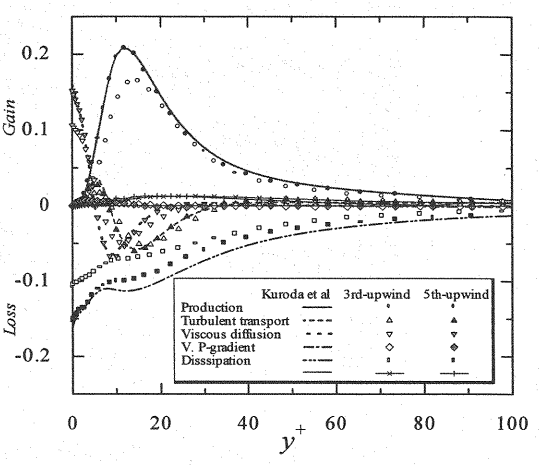

Figure 11 Budget for turbulent energy

from statistical symmetry. This provides evidence that it is possible to obtain information on coherent structures. Both the third- and fifth-order upwind difference schemes reproduce qualitative behavior in the near-wall region, but the third-order upwind results deviate more from the spectral method results.

Figure 10 compares one-dimensional energy spectrum distributions in the buffer layer. The fifth-order upwind difference scheme results show close agreement from the low wave number range to the inertial range, while the third-order results overestimate the u component and underestimate the v and w components. The third-order results show a tendency similar to that of the turbulence intensity distribution, which is thought to indicate that the third-order results reflect the influence of numerical viscosity. It can be seen that in all energy spectra, energy is damped rapidly in the high wave number range. The reason for this is that the viscosity term was evaluated to second-order accuracy. It is likely, therefore, that overall accuracy can be improved by increasing the accuracy of viscosity term evaluation[11].

Figure 11 compares the turbulence energy balance. The generation and dissipation of turbulence energy predominate in the near-wall region, while in the logarithmic law region turbulence energy is damped rapidly to close to local equilibrium. These phenomena have been reproduced accurately. Residual values are slightly on the positive side. This is due to the underestimation of the dissipation factor caused by using the upwind difference scheme. The differences, however, between the third- and fifth-order upwind difference schemes are considerable. This means that information on the near-wall region, which is difficult to obtain through measurement, can be obtained by using a fifth-order upwind difference scheme even with a coarse grid like the one used in the computations performed in this study. The approach using a fifth-order scheme, therefore, is most likely applicable to the evaluation of turbulent flow models in complex flow fields.

Findings of this study show that, the differences between the third- and fifth-order upwind difference schemes are evident. A high-order accurate discretization scheme, therefore, is essential for accurate reproduction of fluid phenomena by using an upwind difference scheme.

Figures 12 and 13 show instantaneous fields at a certain time determined through an analysis using a fifth-order upwind difference scheme. Figure 12 shows the distribution of u^+ fluctuations, in the buffer layer ($y^+ \fallingdotseq 13$). The figure shows that low-speed streaks exist at spacing of about 100 wall units (ν/u_τ). Figure 13 shows u^+ contours in the y-z section at the channel center superposed with instantaneous velocity vectors of v^+ and w^+. This figure indicates that upward flows are formed over the low-speed streaks, and downward flows are formed over the high-speed streaks. Therefore, it is possible to reproduce instantaneous structures including ejections and sweeps with sufficient accuracy.

In conclusion, findings of this study indicate that oscillatory solutions did not occur in any calculations . Findings also indicate the usefulness of an unequally spaced regular grid. It has also been confirmed that application of the central difference scheme to practical calculation is difficult because

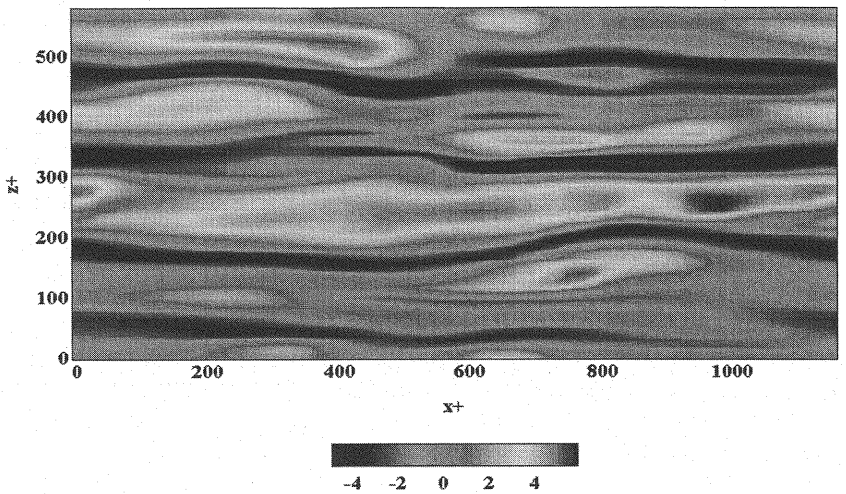

Figure 12 Distribution of velocity fluctuation u^+ (y^+=13)

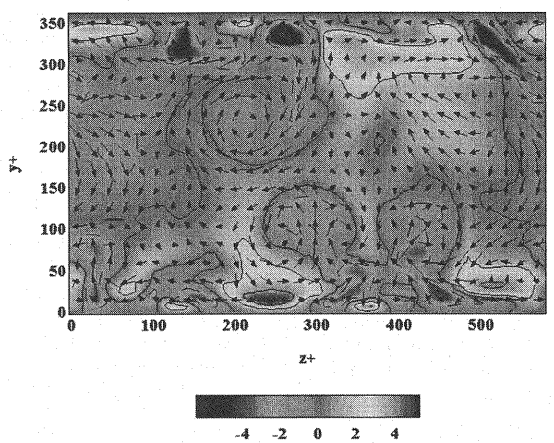

Figure 13 u^+ contours & instantaneous velocity v^+,w^+ (x^+=560)

numerical instability causes divergence of solutions, even when the Courant number is lowered by one order. These results prove that a fifth-order accurate upwind difference scheme, which improves numerical stability while giving highly accurate solutions, contributes to expansion of the scope of application of DNS.

CONCLUSIONS

One-dimensional linear convection problems were studied to investigate the influence of the coupling of temporal and spatial discretization schemes on solutions. Then, as an example, turbulent flows between two parallel plates were simulated by direct numerical simulation combined with an upwind difference scheme to compare the simulation method with the spectral method. From the results thus obtained, the following conclusions were drawn:

1) A second-order accurate Adams-Bashforth method is subject to large temporal phase errors and is

dependent on the Courant number. Care should be taken, therefore, if a long time marching is carried out, as in turbulent flow calculation.

2) The method of analysis coupling a third-order accurate Adams-Bashforth method and a fifth-order accurate upwind difference scheme is almost free from damping and phase errors, and gives numerically stable solutions. When applied to flows between two parallel plates, which is a nonlinear problem, this method of analysis is very useful in engineering because it is highly accurate in comparison to that of the spectral method despite the coarseness of the grid used.

3) Even in an analysis using a regular grid, an unequally spaced grid eliminated spurious errors, and an upwind difference scheme removed aliasing errors.

The method of direct numerical calculation for the Navier-Stokes equations that was developed in this study can be run on a commercially available personal computer. This method of calculation, therefore, has practical applications in engineering.

REFERENCES

1. Kajishima,T. : Conservation properties of finite difference method for convection, Proceedings of JSME, vol.60-574B, pp.2058-2063, 1994. (in Japanese)
2. Kajishima,T. : Upstream-shifted interpolation method for numerical simulation of incompressible flows, Proceedings of JSME, vol.60-578B, pp.3319-3326,1994. (in Japanese)
3. Kasagi,N. : Establishment of the direct numerical simulation data bases of turbulent transport phenomena, 1992. (in Japanese)
4. Kasagi,N. : Direct numerical simulation of turbulence, Science of Machine, vol.45-1, pp.111-115,1993. (in Japanese)
5. Kawamura,T. and Kuwahara,K : Computation of high Reynolds number flow around a circular cylinder with surface roughness, AIAA, 22nd Aerospace Sciences Meeting, paper.84-0340,1984.
6. Kim,J., Moin,P. and Moser,R. : Turbulence statistics in fully developed channel flow at low Reynolds number, J.Fluid Mech., vol.177, pp.133-166, 1987.
7. Kim,J. and Moin,P. : Application of a fractional–step method to incompressible Navier-Stokes equation, J.Comput. Phys., 59, pp.308-323, 1985.
8. Kobayashi,T., Morinishi,Y.:Effect of difference scheme for convective terms within a two-dimensional square cavity, SEISAN KENKYU, vol.40-1, pp.9-15, 1988. (in Japanese)
9. Leonard,B.P. : A survey of finite differences with upwinding for numerical modelling of the incompressible convective diffusion equation, Computational Techniques in Transient and Turbulent Flow, 2, Pineridge Press, 1981.
10. Leonard,B.P. : A stable and accurate convective modelling procedure based on quadratic upstream interpolation, Compt.Methods. Applied Mech.& Eng., vol.19, pp.59-98, 1979.
11. Matsuzaki,K.,Honda,I.,Yoshida,J.,Munekata,M.,Cheng,y. : A study on numerical analysis method of incompressible flows using higher-order accuracy finite difference method, Proceedings of JSME, vol.64-627B, pp.3530-3536,1998. (in Japanese)
12. Miyauchi,Y., Hirata,T., Tanahashi,M.: Direct numerical simulation of three-dimensional homogeneous isotropic turbulence by higher-order finite difference scheme, Proceedings of JSME, vol.61-592B, pp.4400-4405, 1995. (in Japanese)
13. Moin,P.and. Kim,J. : Numerical investigation of turbulent channel flow, J.Fluid Mech. Vol.118, pp.341-377, 1982.
14. Patankar,S.V. : Numerical heat transfer and fluid flow, Hemisphere, 1985.
15. Roache,P.J. : Computational fluids dynamics, Hermosa pub.inc. 1978.
16. Rai,M.M. and Moin,P.: Direct simulation of turbulent flow using finite-difference schemes, J.Comput.Phys.,96, pp.15-53,1991.
17. Suzuki,T. and Kawamura,H.: Consistency of finite-difference scheme in direct numerical simulation of turbulence, Proceedings of JSME, vol.60-578B, pp.3280-3286, 1994. (in Japanese)
18. Tatsumi,T. : Navier-Stokes equation and turbulence, The 44th Nat.Cong.of Theoretical & Applied Mechanics, pp.7-11, 1995. (in Japanese)

APPENDIX – NOTATION

The following symbols are used in this paper :

C	= Courant number ;
F	= flatness factor ;
H	= convection terms ;
p	= pressure ;
Re	= Reynolds number ;
S	= skewness factor ;
t	= time ;
u_τ	= friction velocity ;
u,v,w	= instantaneous velocities in the x,y and z directions ;
$-u'v'$	= Reynolds stress
U,V,W	= mean velocities in the x,y and z directions ;
$\tilde{U}$	= intermediate velocity ;
x,y,z	= coordinates of streamwise,vertical and spanwise direction ;
Δt	= time increment ;
Δx , Δy , Δz	= grid spacings in the x,y and z directions ;
Δx^+, Δy^+, Δz^+	= grid spacings in wall units in the coordinate x,y and z directions ; and
δ	= channel half-width.

The superscript

+	= non-dimensional coordinate normalized by the viscous length.

The subscript

$r.m.s$	= root mean square value.

(Received December 22, 2000 ; revised May 10, 2001)